

Improved resolution and signal-to-noise ratio in laser-ultrasonics by SAFT processing

A. Blouin, D. Lévesque, C. Néron, D. Drolet, J.-P. Monchalain

National Research Council of Canada,
Industrial Materials Institute, 75 de Mortagne Blvd,
Boucherville Qc J4B 6Y4, Canada

alain.blouin@nrc.ca

Abstract: Laser-ultrasonics is an emerging nondestructive technique using lasers for the generation and detection of ultrasound which presents numerous advantages for industrial inspection. In this paper, the problem of detection by laser-ultrasonics of small defects within a material is addressed. Experimental results obtained with laser-ultrasonics are processed using the Synthetic Aperture Focusing Technique (SAFT), yielding improved flaw detectability and spatial resolution. Experiments have been performed on an aluminum sample with a contoured back surface and two flat-bottom holes. Practical interest of coupling SAFT to laser-ultrasonics is also discussed.

© 1998 Optical Society of America¹

OCIS codes: (120.4290) Nondestructive testing; (120.3180) Interferometry

References and links

1. J. Krautkramer and E. Krautkramer, *Ultrasonic Testing of Materials*, (Springer Verlag, New York, 1983).
2. C. B. Scruby, L. E. Drain, *Laser-ultrasonics: techniques and applications*, (Adam Hilger, Bristol, UK, 1990).
3. J.-P. Monchalain, "Progress towards the application of laser-ultrasonics in industry," in *Review of Progress in Quantitative Nondestructive Evaluation*, Vol. 12A, (Plenum, New York, 1993) p. 495.
4. J.-P. Monchalain, "Optical detection of ultrasound," *IEEE Trans. Ultrason. Ferroelectr. Freq. Control*, **33**, 485 (1986).
5. J.-P. Monchalain and R. Héon, "Laser ultrasonic generation and optical detection with a confocal Fabry-Perot interferometer," *Mater. Evaluation*, **44**, 1231 (1986).
6. P. Delaye, A. Blouin, D. Drolet, L.-A. de Montmorillon, G. Roosen, J.-P. Monchalain, "Detection of ultrasonic motion of a scattering surface by photorefractive InP:Fe under an applied field," *J. Opt. Soc. Am. B*, **14**, 1723 (1997).
7. P. Delaye, A. Blouin, D. Drolet, J.-P. Monchalain, "Heterodyne detection of ultrasound from rough surfaces using a double phase conjugate mirror," *Appl. Phys. Lett.*, **67**, 3251 (1995).
8. P. V. Mitchell, G. J. Dunning, S. W. McCahon, M. B. Klein, T. R. O'Meara, D. M. Pepper, "Compensated High-bandwidth laser ultrasonic detector based on photo-induced emf in GaAs," in *Review of Progress in Quantitative Nondestructive Evaluation*, Vol. 15, (Plenum, New York, 1996) p. 2149.
9. P. W. Lorraine, R. A. Hewes and D. Drolet, "High resolution laser ultrasound detection of metal defects," in *Review of Progress in Quantitative Nondestructive Evaluation*, Vol. 16, (Plenum, New York, 1997) p. 555.
10. K. Mayer, R. Marklein, K. J. Langenberg and T. Kreutter, "Three-dimensional imaging system based on Fourier transform synthetic aperture focusing technique," *Ultrasonics*, **28**, 241 (1990).
11. L. J. Busse, "Three-dimensional imaging using a frequency-domain synthetic aperture focusing technique," *IEEE Trans. Ultrason. Ferroelectr. Freq. Control*, **39**, 174 (1992).
12. T.-J. Teo and J. M. Reid, "Multifrequency holography using backpropagation," *Ultrasonic Imaging*, **8**, 213 (1986).

¹ This work has been performed in a Canadian Government laboratory and therefore the copyright for this article belongs to the Government of Canada.

1. Introduction

Laser-ultrasonics is a novel technique which marries ultrasonics and optics and extends the capabilities of optics for inspecting materials. Optics is limited in the sense that it cannot probe below the surface of opaque materials, which is the case of most industrial materials. The conversion of the energy of a pulsed laser to ultrasound and the optical detection of ultrasonic waves allow to probe deep inside opaque materials to find hidden flaws. To introduce the subject of this paper, we provide below some background information on ultrasonics first, then on laser-ultrasonics.

1.1 Ultrasonics

Ultrasonics is well recognized to be a powerful non-invasive diagnostic technique. Everyone is familiar with its use in medicine, particularly to observe a fetus in the womb of his mother. Its use for imaging through opaque materials, particularly to find flaws like cracks, disbands, or delaminations is also well known, and uses the same principle and technology [1]. In both fields of application, the ultrasonic waves are usually produced by making a piezoelectric ceramic transducer to vibrate under an electrical impulse. The waves are then coupled to the object (or body) under inspection by using a liquid or viscous film to establish a contact between the emitting transducer and the object. A common practice consists of immersing the object in a water bath or to use water jets. Usually, the emitting transducer is also used as receiver of the ultrasonic echoes, i.e. the waves reflected by acoustic discontinuities inside the inspected object, and produces electrical signals indicative of the discontinuities. This ultrasonic technique provides not only information on the presence of such discontinuities, but also an indication on their depth, deduced from the arrival time of the echoes and the knowledge of the acoustic wave velocity. By mechanically scanning the emitting/receiving transducer, the object can be mapped out throughout its entire volume and the information displayed as B-scans or C-scans. B-scans are planar cuts through the material and indicate directly the depth of the discontinuities that are found. C-scans are more like views from the surface and provide depth information by using a color or gray scale code. The coding may be associated either to the arrival time of echoes or their amplitude to enhance some features.

The method of generation and detection of ultrasound using piezoelectric transducers that are coupled to the inspected object may be called *conventional ultrasonics*. Such a technique, because it requires fluid coupling cannot obviously been applied at elevated temperatures. Also if the temperature exceeds the Curie temperature of the transducer material, the transducer ceases to be piezoelectric and operational. On the other hand, being able to use ultrasound at elevated temperatures could be of far reaching importance, since all metals and ceramics are processed at these temperatures. Another limitation of conventional ultrasonics is the difficulty to inspect curved objects. Since the piezoelectric transducer works as a piston, emitting and receiving a wave from its whole surface, its orientation with respect to the surface of the inspected part is important. As a matter of fact, the angular tolerance is typically a few degrees and in the case of curved surfaces, the transducer should be mounted on a robotic system to follow the contour. These limitations are circumvented by using lasers both for generation and detection of ultrasound, a technique called *laser-ultrasonics* [2,3].

1.2 Laser-ultrasonics

Laser-ultrasonics uses one laser with a short pulse for generation and another one, long pulse or continuous, coupled to an optical interferometer for detection. In this case there is obviously no need of fluid coupling and transduction can even be performed in vacuum. By relying on optics for providing the transduction of ultrasound, laser-ultrasonics brings

practical solutions for testing at a large standoff distance, inspection of moving parts on production lines and inspection in hostile environments [3]. Laser-ulasonics features also a large frequency bandwidth, which is important for numerous applications involving material characterization.

Generation of ultrasound can be performed either in the ablation or thermoelastic regime. In the first case, a sufficiently strong laser pulse provides vaporization or ablation of the surface. The recoil effect following material ejection off the surface produces strong longitudinal wave emission perpendicular to the surface. In the thermoelastic regime, a laser source is chosen with a wavelength penetrating significantly below the surface. This penetration is easily achieved with many polymer-based materials and materials with painted surfaces. It produces a buried source and a constraining effect of the material above it, which increases longitudinal ultrasonic emission along the normal.

With laser generation, the ultrasonic source is located at the surface of the part and follows automatically the contour. Furthermore, the conditions of generation mentioned above favors emission of waves propagating normally to the surface, independently of the incidence angle of the laser beam. Detection of the reflected or scattered ultrasonic waves is also performed from the surface with the second laser and does not require any alignment. This obviously assumes that enough light is collected, by using a detection laser of appropriate power and a collecting aperture of sufficient size. This important feature of laser-ulasonics can be viewed in Fig. 1 where the beams are simply scanned over the surface.

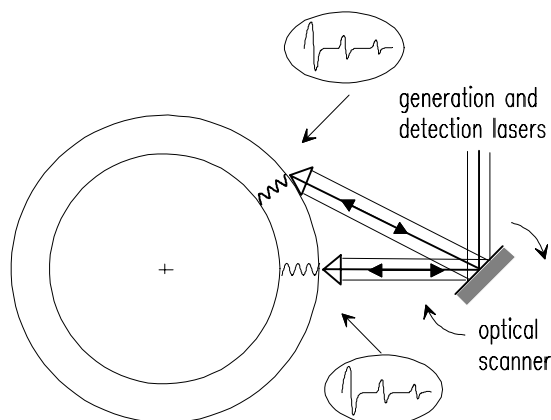


Fig. 1. Laser-ultrasonic inspection of a pipe. Generation is assumed in a regime which produces essentially normally propagating ultrasonic waves. The arrows indicate the generation and detection laser beams at two locations determined by the optical scanner. The inserts indicate schematically the ultrasonic echoes as observed on an oscilloscope.

For the optical detection of ultrasound, the small phase or frequency shift (Doppler effect) in the scattered light induced by the ultrasonic surface motion is detected by an interferometric system. Note that the surface of the industrial materials to be inspected is usually rough which leads to a scattered beam with speckle. For applications in industry, especially if the inspected part is scanned or is moving, a detection scheme which is independent of the speckle or integrates over the whole speckle field is needed. This requires to produce inside the interferometer a reference wave which is adapted or matched the incoming speckled wave scattered off the surface. Two approaches can be followed to reach this goal, a passive approach, based on time-delay interferometry and an active one, using nonlinear optics to provide wavefront adaptation. Regarding time-delay interferometry (also

called velocity interferometry) [4], the most useful system being used presently is the confocal Fabry-Perot, operating either in transmission or in reflection [5]. Such a confocal Fabry-Perot operated in the transmission mode was used for the work reported below. The active approach developed so far has been based on wave mixing in photorefractive crystals. Characteristics of adaptive interferometers using two-wave mixing in semiconductor photorefractive crystals [6] and based on a double phase conjugate mirror [7] were reported. Another scheme based on the photo-induced electromotive force in semi-insulating crystal was also developed [8]. All these interferometric schemes, either active or passive, provide a relatively large etendue or throughput, corresponding to integration over a broad section of the speckle field. For example, a meter-long confocal Fabry-Perot can demodulate all the light transmitted by a one-millimeter core fiber.

Regarding the detection of small defects, ultrasonics or laser-ultrasonics has similar limitations as optical microscopy, caused by the wave nature of the interrogation and diffraction effects. In particular, in laser-ultrasonics, the spatial resolution is dependent upon the spot sizes of the generation and detection beams at the surface of the part, and could be inadequate for detecting small and deep flaws. The use of a broad laser spot to produce an ultrasonic beam with little divergence gives a resolution essentially limited by this spot size. On the other hand, if the laser beam is focused onto a small spot, a strongly diverging wave is obtained, leading also to poor resolution for the detection of deep flaws. In conventional ultrasonics, the detection of small buried defects is achieved by focusing the acoustic field with lenses or curved transducers. The approach is similar to one used in optical microscopy where a high numerical aperture lens is used to detect small features. Alternatively a computational technique that basically consists in performing the focusing numerically can be used. This method, known as the Synthetic Aperture Focusing Technique (SAFT) [9], is traditionally implemented by scanning a focused piezoelectric transducer over the surface of the specimen and then processing the collected data array. In this paper we are reporting the use of laser-ultrasonics for collecting the ultrasonic data, with the advantages of easy scanning and modification of the spot size of the laser beams. Two versions of SAFT applied to laser-ultrasonic data are presented: 1) the intuitive but heuristic conventional algorithm in the time domain and 2) the computationally efficient algorithm in the Fourier domain (F-SAFT). These processing techniques are then applied to data collected on an aluminum test specimen with a contoured back surface and two flat-bottom holes drilled in it. It will be shown that SAFT data processing improves the ability to detect and size defects.

2. Principle of SAFT processing

We assume that the generation and detection beams are focused at the same location onto the surface. By scanning the beams or moving the part fixed on an X-Y translation table with discrete and equal steps, a 2-D mesh at the surface $z = 0$ of the specimen is obtained. As shown in Fig. 2, if a pointlike flaw is present at point C located at a depth z within the sample, this flaw re-radiates the acoustic field originating at point M_i . The acoustic signal $S(M_i, t)$ received at any point M_i in the measurement mesh exhibits a peak at time $t = 2d_i / v$, where v is the longitudinal acoustic velocity in the material and d_i the distance CM_i . Consequently, the summation:

$$\Sigma(C) = \sum_{M_i \in \text{mesh}} S\left(M_i, t = \frac{2d_i}{v}\right) \quad (1)$$

separates the points C where superpositions build up and flaws are present, from the points C where no coherent superposition occurs and the material is sound. Moreover, the function

$\Sigma(C)$ increases the signal-to-noise ratio for the detection of flaws by the factor \sqrt{N} , where N is the number of points M_i in the measurement mesh aperture (the synthetic aperture).

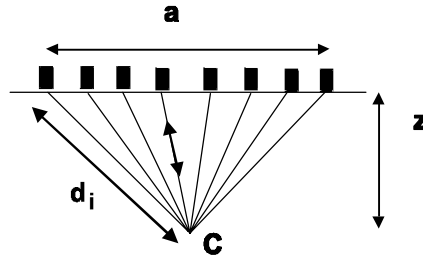


Fig. 2. Principle of SAFT.

This simple reconstruction algorithm is a phase correction technique since it performs the summation of signals shifted in time. The time shift of each signal is a function of the point M_i where the signal is collected and of the point C where one wants to check the presence of a flaw. It can be shown that the lateral and depth resolutions obtained from the SAFT algorithm are respectively:

$$\Delta x \approx v \Delta t \frac{z}{a}, \quad \Delta z \approx \frac{v \Delta t}{2} \quad (2)$$

where Δt is the ultrasonic pulse duration and a is the dimension of the synthetic aperture. While maintaining the depth resolution of the conventional pulse-echo method, the SAFT processing leads to improved lateral resolution. In practice, the strength of ultrasonic wave emission and the detection sensitivity both decrease away from the normal to the surface, so that the total opening angle of the synthetic aperture is limited to roughly 60° or $a \sim z$.

This data processing approach, while straightforward in its principle and implementation, is not very efficient and is very computation intensive. An alternate and better approach is to perform the data processing in the Fourier domain (F-SAFT) and to benefit from the Fast Fourier Transform (FFT) algorithm to reduce the processing time. The F-SAFT is a backpropagation technique which is based on the angular spectrum method of the scalar diffraction theory. Starting from the acoustic field $S(x, y, z = 0, t)$ at the sample surface of the measurement mesh (axes x and y), a 3-D Fourier transformation is performed with respect to variables (x, y, t) into a 3-D Fourier space represented by variables (σ_x, σ_y, f) . Physically this consists in representing each acoustic field at f by a superposition of plane waves with wavenumbers of components σ_x, σ_y . Then, assuming a flaw located at depth z , the transformed field $\bar{S}(\sigma_x, \sigma_y, z = 0, f)$ is backpropagated to the source plane as follows:

$$\bar{S}(\sigma_x, \sigma_y, z, f) = \bar{S}(\sigma_x, \sigma_y, 0, f) \exp\left(2\pi i z \sqrt{\frac{f^2}{(v/2)^2} - \sigma_x^2 - \sigma_y^2}\right) \quad (3)$$

The exponential function in Eq. (3) is called the backpropagator and is actually a phase shifter for the propagating waves. For simultaneously scanned generation and detection (see Fig. 2), the acoustic propagation distances are doubled and this is accounted for in the

backpropagator by a velocity reduced by the factor of 2. After backpropagation to the source plane, a summation over temporal frequency components f is performed as follows:

$$\bar{\Sigma}(\sigma_x, \sigma_y, z) = \sum_{f \in \Omega} \bar{S}(\sigma_x, \sigma_y, z, f) \quad (4)$$

where Ω is the actual frequency bandwidth of the system. Finally, an inverse 2-D Fourier transformation of $\bar{\Sigma}(\sigma_x, \sigma_y, z)$ with respect to variables (σ_x, σ_y) into (x, y) yields the function $\Sigma(x, y, z)$. A point C (at position x, y, z) will correspond to a flaw if the summation Σ at this point exhibits a peak. This processing method is also presented in more details in references [10-12].

3. Laser-ultrasonic setup and results on test specimen

The generation laser was a short pulse (≈ 5 ns) Q-switched Nd:YAG laser operating on its fourth harmonic and producing slight ablation at the sample surface. A single mode, highly stable, long pulse (50 μ s) Nd:YAG laser operated on its fundamental wavelength of 1.064 μ m was used for the detection of ultrasound. The light of the detection laser scattered off the surface of the sample was sent to a confocal Fabry-Perot interferometer. The two laser beams were focused onto the flat surface of the specimen at about the same location. For practical reasons, an X-Y translation table was used to move the tested parts instead of scanning the laser beams.

The test specimen was made from a 40 x 16 x 7 mm aluminum block. One of its surface was machined to obtain a non-planar back surface, as shown in Fig. 3. To simulate buried flaws, two flat-bottom holes of 1.0 and 0.5 mm in diameter and 1.5 mm deep were drilled from the back surface. The step size of the scan was 0.1 mm and the scanned area was about 25.4 x 10 mm. The generation and detection spot sizes were 0.1 mm and 0.3 mm respectively. For each node M_i of the measurement mesh, an ultrasonic signal was collected, digitized and stored in the computer memory. The data was processed by the most efficient of the two algorithms mentioned above, the F-SAFT algorithm.

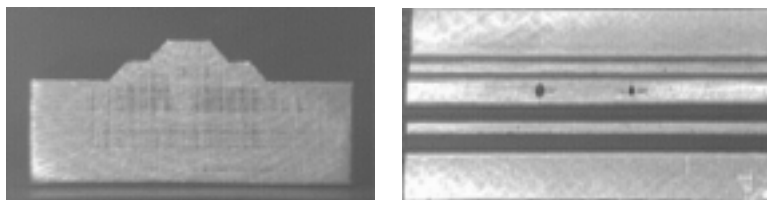


Fig. 3. Photos of the test specimen.

An improvement to the raw data was first obtained by applying a high pass filter with a cut-off frequency of 4 MHz on the signals, to remove any offset and low-frequency surface waves. The filtered data were then processed using the F-SAFT algorithm and Fig. 4 shows C-scans of both the filtered and F-SAFT processed data. Each C-scan was obtained by selecting the peak-to-peak value from each ultrasonic signal in a narrow gate at depths between 5.2 and 5.7 mm corresponding to the bottom of the holes. The profiles along a line crossing the holes on these C-scans are also shown. When compared to the filtered data, the F-SAFT processed data show strong improvements of the detectivity and of the lateral resolution of the flat-bottom holes. From the data, estimates are given in Table 1 of the

signal-to-noise ratio, apparent diameter and bottom location for the two holes. The temporal width of the ultrasonic pulse extracted from the backwall echo was $\Delta t = 90$ ns, which yields lateral and depth resolution estimates from Eq. (2) of $\Delta x \approx 0.6$ mm and $\Delta z \approx 0.3$ mm, in agreement with the observations reported in Table 1.

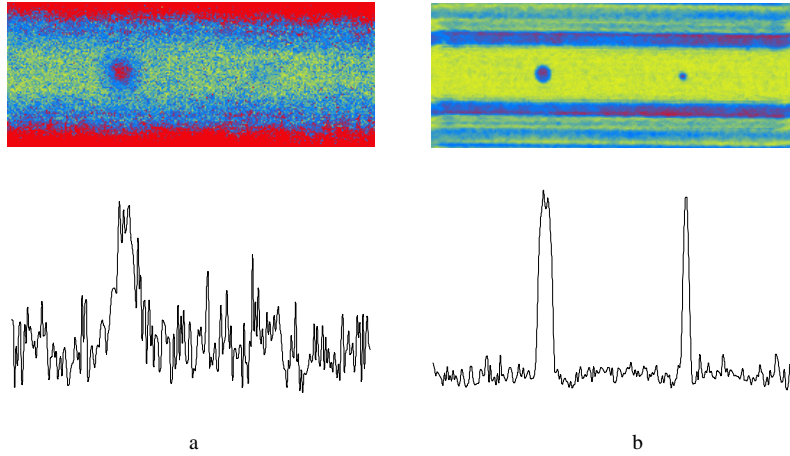


Fig. 4. C-scans and profiles of the a) filtered and b) F-SAFT data.

Table 1. Comparison of SNR, apparent diameter and depth resolution (DR).

	SNR (dB)	Diameter (mm)	DR (mm)
Filtered data			
Hole 1.0 mm dia.	6	2.0	0.3
Hole 0.5 mm dia.	2	1.7	-
F-SAFT data			
Hole 1.0 mm dia.	23	1.0	0.3
Hole 0.5 mm dia.	23	0.5	0.3

B-scans of the filtered and F-SAFT processed data are shown in Figs. 5a and 5b. These two images show that SAFT processing can also be used to resolve the contour of a non-planar back surface. In Figs. 5c and 5d, the B-scans are taken through the 0.5 mm diameter flat-bottom hole and both the contoured back surface and the flat-bottom holes are still resolved. With prior knowledge of the part shape, the laser-ultrasonics SAFT technique can also be applied to samples with contoured front surfaces. Quite clearly from these results, F-SAFT processing has brought a very significant improvement to defect detection and sizing and to the resolution of the backwall contour.

It should be mentioned however that the SAFT processing cannot be performed in real-time. As an example, the F-SAFT processing time for this experiment was about 20 min on a PC Pentium 200 MHz for a data set of 255 x 101 ultrasonic signals of 301 datapoints ($\approx 7.7 \times 10^6$ datapoints) and for reconstruction at 151 depths. In practice, a

compromise has to be found for the scanning step size, between the smallest detectable defect and the processing time. As an example, a subset of 63 x 25 ultrasonic signals from the previous data was taken corresponding to a step of 0.4 mm (compared to 0.1 mm for the original one) and analyzed to see the influence on flaw detectivity. Fig. 6 shows C-scans and profiles when the data subset is processed using the F-SAFT algorithm, including or not the improvement given by an interpolation algorithm. The F-SAFT processing allows detection of both the 1.0 and 0.5 mm diameter holes with a 0.4 mm step size, but the smaller defect appears clearly only when used in combination with suitable interpolation. Here, an interpolation algorithm based on FFT is used and embedded in the F-SAFT processing. For each depth z , it simply consists in padding the function $\bar{\Sigma}(\sigma_x, \sigma_y, z)$ with zeros prior to its inverse 2-D Fourier transformation, yielding the function $\Sigma(x, y, z)$ at intermediate points. While less accurate than in Fig. 4b, the resulting C-scan in Fig. 6 appears quite acceptable taking into account the reduction factor of 16 in data collection time and 5 in processing time. Other step sizes were tested with the same approach, indicating that the minimum step size required to achieve adequate resolution is approximately equal to the defect size.

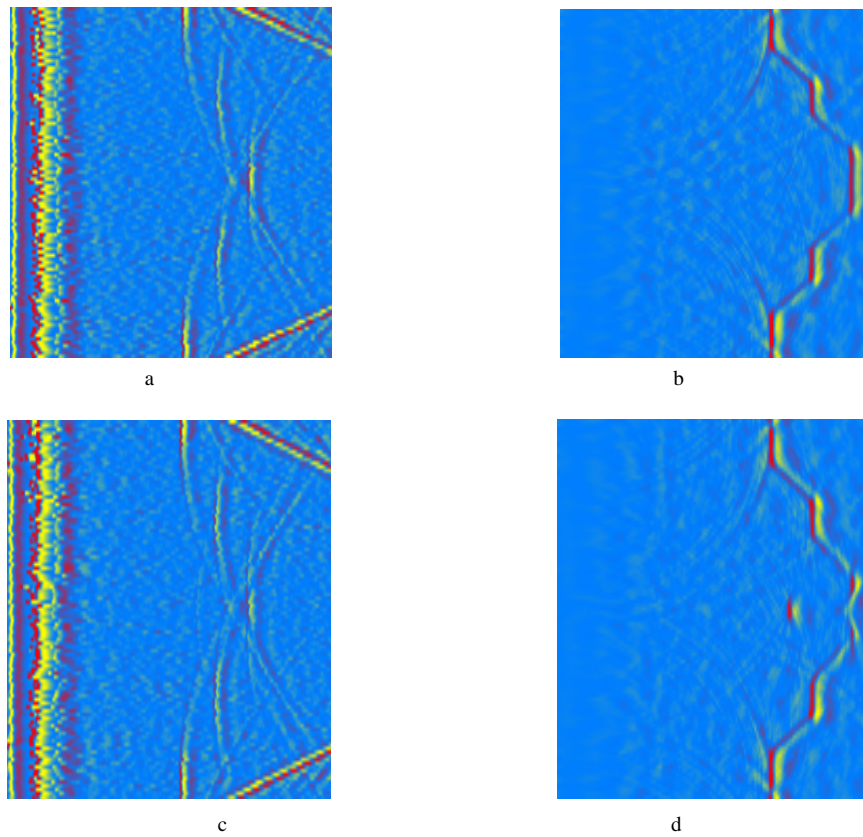


Fig. 5. B-scans of filtered (a,c) and F-SAFT processed data (b,d) from the aluminum test specimen. B-scans of figs. 5c and 5d were taken through the 0.5 mm dia. flat-bottom hole.

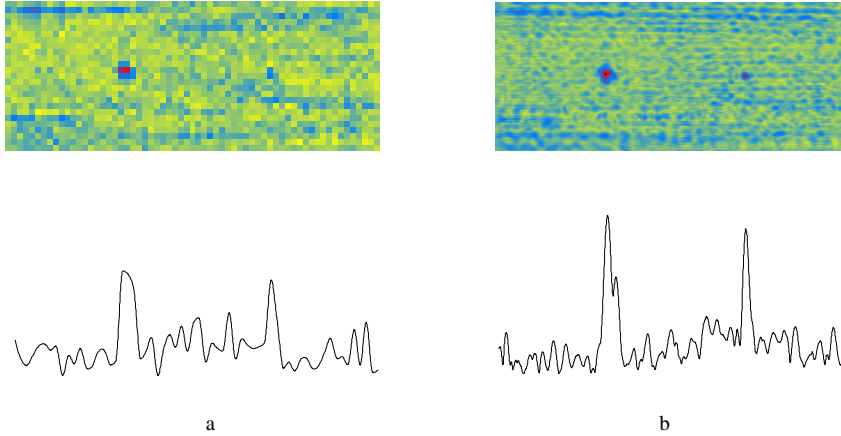


Fig. 6. C-scans and profiles from a subset of data corresponding to a 0.4 mm step: F-SAFT processed data a) without interpolation and b) with interpolation.

4. Conclusion

We have reported on the use of SAFT data processing to improve the spatial resolution and the detectability of laser-ultrasonics. The laser-ultrasonic technology is well suited for SAFT data acquisition since laser beams are easily scanned and their spot sizes easily modified. Moreover, laser-ultrasonics is a non-contact inspection technique that can be used on parts of complex shapes. In our setup, the two laser beams, which act as the acoustic source and receiver, were focused onto the surface at about the same location and the parts were moved. Other configurations where the two laser beams are offset from each other or are not simultaneously scanned can also be easily implemented. This work has shown that SAFT data processing results in an improvement of the lateral resolution of laser-ultrasonics. In addition, the averaging performed by SAFT processing increases the capability of defect detection. We have also shown that SAFT processing can be used to resolve the contour of a non-planar back surface. With prior knowledge of the part shape, the laser-ultrasonic SAFT technique can also be applied to samples with non-planar front surfaces.